J Paleolimnol
https://doi.org/10.1007/s10933-023-00280-1

ORIGINAL PAPER

A palaeoecological study investigating the impacts of multiple tephra depositions on a lacustrine ecosystem in Northeast China, using diatoms as environmental indicators

Yuqiao Natalie Deng · Patrick Rioual · Vivienne J. Jones · Chunqing Sun · Jens Mingram

Received: 1 November 2022 / Accepted: 19 January 2023

Abstract Tephra layers are common in lake sediments and although they have often been used as chronological controls, few studies have investigated the impacts of past tephra depositions on lake ecosystems (Tephropalaeoecology). For the first time we systematically assess how different types of tephra layers vary in their ecological impact on the same lacustrine system. We use a diatom-based tephropalaeoecological approach to infer the impacts of five tephra deposits on Lake Sihailongwan, a well-studied volcanic lake in Northeast China, over the past 30,000 years. The five tephra layers (including two micro-tephras) have varying thicknesses and were deposited in time periods with different climatic conditions. Changes in diatom communities and chrysophyte-cyst concentrations between pre- and post-tephra samples were used to infer changes in lake conditions and highlight the importance of lake background conditions in mediating the impact of tephra. While the two micro-tephra layers did not cause observable changes, the three thicker tephras induced pronounced changes in lake conditions and thus diatom communities. The two thick tephras deposited in more eutrophic and warmer lake conditions caused larger responses from diatoms. We argue that water-column phosphorus decreased due to reduced sediment–water-phosphorus loading as thick tephra layers formed an impermeable layer at the lake bottom. This is supported by a decrease in total diatom concentration and a decline in high phosphorus-requiring taxa such as *Discostella stelligeroides* and *Stephanodiscus minutulus* as well as modern limnological observations which showed that groundwater influxes from the lake bottom are the main source of nutrients to

Supplementary Information The online version contains supplementary material available at https://doi.org/10.1007/s10933-023-00280-1.

Y. N. Deng (✉) · V. J. Jones
Environmental Change Research Centre, Department of Geography, University College London, North West Wing, Gower St, London WC1E 6BT, UK
e-mail: natalie.deng.19@ucl.ac.uk

V. J. Jones
e-mail: vivienne.jones@ucl.ac.uk

P. Rioual
Key Laboratory of Cenozoic Geology and Environment, Institute of Geology and Geophysics, Chinese Academy of Sciences, Beijing 100029, China
e-mail: prioual@mail.iggcas.ac.cn

P. Rioual
CAS Center for Excellence in Life and Paleoenvironment, Beijing, China

C. Sun
Division of Cenozoic Geology and Environment, Institute of Geology and Geophysics, Chinese Academy of Sciences, Beijing 100029, China
e-mail: suncq@mail.iggcas.ac.cn

J. Mingram
GFZ German Research Centre for Geosciences, Telegrafenberg C323, 14473 Potsdam, Germany
e-mail: jens.mingram@gfz-potsdam.de

Published online: 02 March 2023

the lake. By contrast, the thick tephra deposited in more oligotrophic and colder lake conditions caused less conspicuous changes. When the lake was already low in phosphorus, diatoms did not respond to a further decline in phosphorus but rather responded to the minor increase in silica from the dissolution of tephra particles in the water column. This was inferred from the slight increases in overall diatom concentration and opportunistic taxa such as *Pantocsekiella comensis* f. *minima*. Diatom analysis of the post-tephra sediments above the three thick tephras showed that the aquatic ecosystem did not completely recover, indicating the long-lasting effects of these thick tephras and shifts to new lake-ecosystem equilibria.

Keywords Palaeolimnology · Maar lake · Volcanic eruption impacts · *Pantocsekiella comensis* f. *minima* comb. nov.

Introduction

The majority of palaeolimnological studies are concerned with longer-term perturbations and very few try to deal with transient environmental disturbances such as volcanic eruptions (Payne and Egan 2019). Palaeolimnology provides a useful tool to investigate past eruptions that can be recorded in lake sediments as tephra layers. Tephra deposits are commonly found in lake sediments around the world and are used frequently as marker layers in sediment cores and when they can be dated, they are the basis for tephrochronology (Lowe 2011), but their impacts on the ecology and functioning of the lakes themselves have often been overlooked (Urrutia et al. 2007). However, we can use the long-term records in lake sediments to identify and reconstruct the impacts of volcanic eruptions. This is valuable for understanding the eruptive history of a region and assessing the response, recovery, equilibrium, sensitivity and adaptability of a lake system to abrupt perturbations (Payne and Egan 2019).

Tephra is unconsolidated pyroclastic material blown into the air by volcanic eruptions (Arnalds 2013). Once in the air, tephra can disperse and deposit on different environments proximal or distal to the volcanic source. Tephra depositions in water bodies can alter the chemical and physical properties of aquatic systems, impacting aquatic organisms by changes in nutrients, habitats and living conditions (Ayris and Delmelle 2012; Egan 2016). In volcanically active regions, tephra depositions can be the dominant drivers of change in lacustrine ecosystems (Michelutti et al. 2015). Physically, tephra can directly blanket and smother habitats and organisms. Tephra particles in lakes can increase water turbidity (Mayr et al. 2019), reducing light penetration hence autochthonous photosynthesis (Burwell 2003). The formation of a water–sediment-interface barrier in the bottom of lakes can occur (Eastwood et al. 2002), as tephra tends to cement and form an impermeable layer when reacting with water (Egan et al. 2018). This disturbs nutrient exchange between the sediment and the water, particularly reducing the possibility for nutrients to diffuse into the water column from the bottom sediment (Harper et al. 1986; Lotter et al. 1995; Hutchinson et al. 2019). On the other hand, silica (SiO_2) can leach from the tephra particles into the water column (Barker et al. 2000), fertilising siliceous biological production (Hickman and Reasoner 1994; Hardardóttir et al. 2001).

Diatoms are ubiquitous unicellular algae found in almost every aquatic ecosystem (Jones 2013). As one of the main aquatic primary producers, diatoms are sensitive to changes in their environments (Mackay et al. 2003). This together with their often excellent preservation in sediments arising from their siliceous frustules, make them robust biological indicators for reconstructing past aquatic conditions and tracking ecosystems' responses to perturbations (Lowe and Walker 2015). Accordingly, diatoms are ideal proxies for tracking the impacts of tephra depositions on lacustrine systems. Studies have demonstrated that tephra depositions can induce changes in diatom populations and lake systems in physical and chemical ways. The more widely documented changes include increase in water turbidity (Mayr et al. 2019), benthic habitat smothering (Hickman and Reasoner 1994), increase in lake SiO_2 from tephra-particle dissolutions (Barker et al. 2000), as well as occurrence of a water–sediment-interface barrier which restricts P-loading (Harper et al. 1986; Lotter et al. 1995; Eastwood et al. 2002; Egan et al. 2018; Hutchinson et al. 2019). Chrysophytes, another widespread group of algae that produce siliceous resting cysts which are also well preserved in sediments (Adam and Mahood 1981; Sandgren 1991; Pla et al. 2003),

although less extensively used than diatoms, can also be employed as indicators of a lake's condition, and can complement diatom analysis.

There is a lack of consensus on diatoms and lakes' responses to tephra depositions and the impact duration and time required for a lake system to recover to the pre-perturbation state (Wutke et al. 2015). Some studies have suggested very brief impact durations in which ecosystems were able to return to their pre-tephra states in 5–20 years (Lotter and Birks 1993; Hutchinson et al. 2019), while other studies have indicated much longer recovery periods (200–500 years; Hickman and Reasoner 1994; Egan et al. 2018). Thus, the impacts of tephra on lakes are likely to be site-specific. Additionally, there are studies that have found no correlations or significant changes between diatom communities and tephra deposition. For instance, Hickman and Reasoner (1994) examined diatoms in some shallow Canadian lakes and only found minor diatom concentration decreases not large enough to be attributed to tephra depositions. Similarly, Abella (1988) found no clear signals in total diatom abundance and productivity following tephra deposition in Lake Washington (USA). The reason for this could be that these tephras were deposited in a quantity not large enough to induce ecological responses (Telford et al. 2004), or because the lake background conditions were already experiencing other non-volcanic fluctuations.

This study investigated the impacts of five temporally and physically (as measured by thickness) distinct tephras on a lake in northeast China (Lake Sihailongwan) during the past 30,000 years, using diatoms and chrysophytes as indicators for changing aquatic conditions. By comparing across multiple tephra layers from the same lake, site consistency can be ensured as the lake-catchment geology and morphology have been constant throughout, although climate change will have occurred. Accordingly, the aims were to:

(1) Identify the presence or absence of significant changes in the diatom assemblages pre- and post-tephra deposition.
(2) Examine differences in lake response and recovery to tephras of different thicknesses and under different climatic regimes.

Study site

Northeast China is an area with widespread Cenozoic volcanism. Due to the deep subduction of the Pacific plate slab, several intra-plate volcanic belts were created in this region (Duan et al. 2009). The most intense one is the Changbai Mountain Volcanic Belt. Located in the middle of this volcanic belt are the Changbai Mountains and the Longgang Volcanic Field (LVF; Wang et al. 2001). The LVF (Fig. 1) is a volcanic field located in the south of Jilin Province characterised by alkali-basaltic rocks covering an upper Archean basement (Frank 2007). It contains 164 volcanic cones and 8 maar lakes (Liu and Taniguchi 2002). The maar lakes are meso-oligotrophic, remote and have water supplied mainly from groundwater, runoff and precipitation. They are also relatively well-buffered by abundant bicarbonate ions (HCO_3^-; Yan 1998).

Sihailongwan (42°17′13.8′ N 126°36′ 07.0′ E) is one of the 8 crater lakes in the LVF. It has a U-shaped basin (Zhao and Hall 2015) and is located ~ 20 km southeast of the Jinlongdingzi Volcano (Liu et al. 2009; Fig. 1). Sihailongwan has a water surface area of 0.5 km^2, a maximum water depth of 50 m (Chu et al. 2005) and a small non-calcareous 0.7 km^2 catchment delimited by the maar rim, which rises 120 m above the lake-water surface (Mingram et al. 2018). The lake-water level is controlled by precipitation and groundwater with no surface inflow/outflow (Rioual et al. 2016; Mingram et al. 2018). Sihailongwan overturns twice a year in spring and autumn (Chu et al. 2005) and has a distinct thermal stratification during the summer (Mingram et al. 2004). A thick ice cover forms on the lake surface in winter (Chu et al. 2005). The modern regional climate exhibits strong Asian monsoon-controlled seasonality, manifested by cold dry winters and warm wet summers (Chu et al. 2005; Stebich et al. 2009). Sihailongwan has laminated lake sediments with little bioturbation (Zhao et al. 2017; Wu et al. 2019) due to the presence of lake-bottom anoxia arising from the distinct maar morphology (Mingram et al. 2004).

The dominant nutrient (Si and P) influx into Sihailongwan is via groundwater (Schettler et al. 2006a), shown by the nutrient-concentration measurements in groundwater and the vertical lake-nutrient profiles (Fig. 2). Si and P are the main limiting factors currently affecting primary/photosynthetic productivity

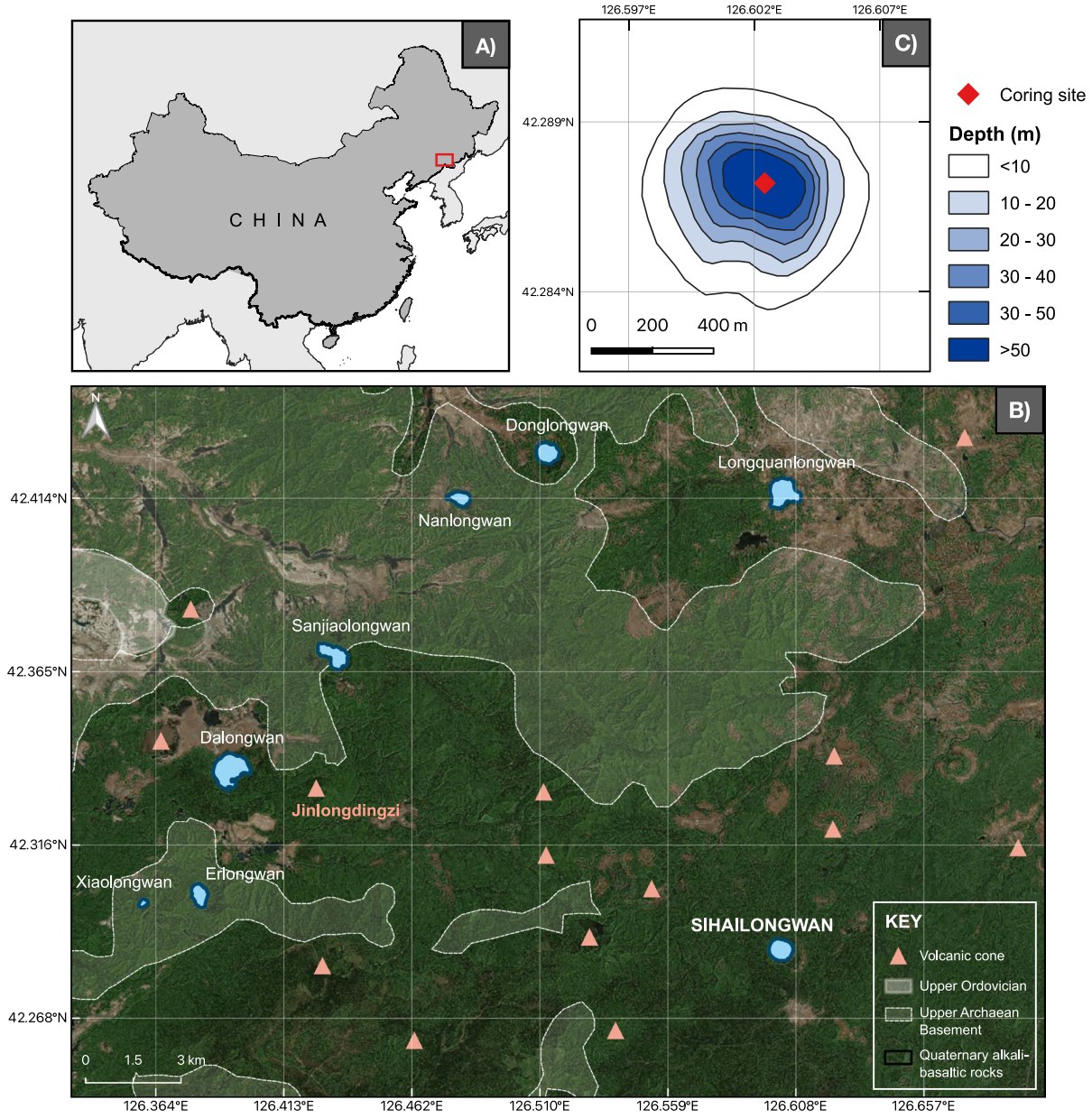

Fig. 1 Study area **A** location map of the Longgang Volcanic Field (LVF) as indicated by the red rectangle. **B** map of the local area, adapted from Schettler et al. (2004), showing the position of Sihailongwan, seven other crater lakes in the LVF, major volcanic cones and local geology. The position of the Jinlongdingzi Volcano is derived from Liu et al. (2009). **C** lake bathymetry of Sihailongwan and the coring site adapted from Chu et al. (2005)

in the lake (Schettler et al. 2006a). Sihailongwan's nutrient condition is highly dependent on the climate. When warmer and wetter conditions prevail, groundwater influx increases, supplying more nutrients to the lake. The dissolved nutrients in groundwater mostly come from local organic and siliciclastic materials originated within the lake catchment (especially from the weathering of alkali-basaltic pumice tuff). When colder conditions prevaile, remote aeolian detrital material deposited from beyond the LVF constitutes the majority of the lake-nutrient input (Schettler et al. 2006a; Zhu et al. 2013).

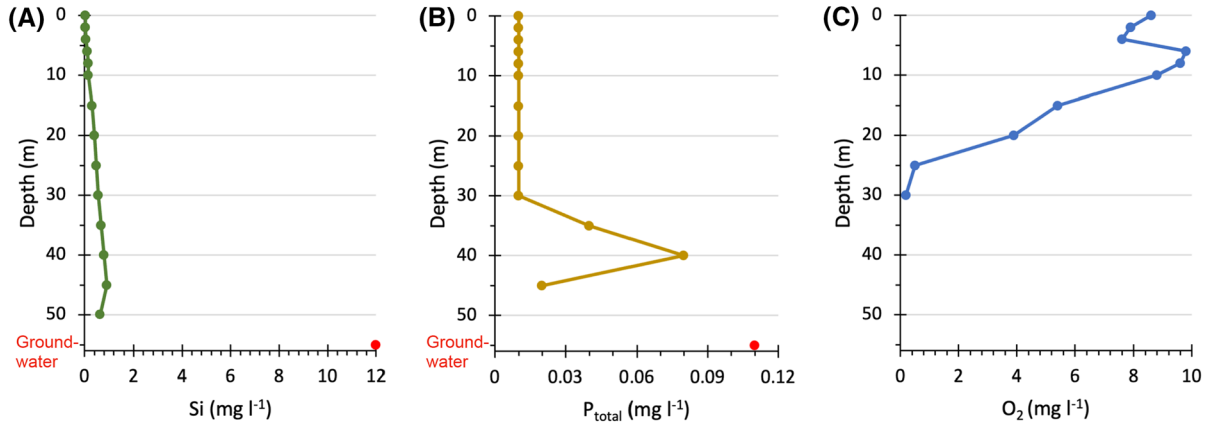

Fig. 2 Vertical profile of modern hydrochemical data in Sihailongwan showing concentrations of **A)** Silica (Si), **B)** Phosphorus (P_{total}), and **C)** Dissolved oxygen (O_2). The red dots are measurements from groundwater samples. Si and P_{total} decrease upward along the water column, while the groundwater concentrations largely exceed those of the lake. O_2 concentration increase upward along the water column with near zero concentration at 30 m, indicating lake-bottom anoxia. All measurements were taken in June 2001 (Schettler et al. 2006a)

Much of the autochthonous sediment fraction constitutes of biogenic silica ($bSiO_2$) from diatom production (Schettler et al. 2006a). Sediment-trap data have revealed that in the present conditions, diatom-flux peaks in autumn after the summer-maximum precipitation (Chu et al. 2005; Schettler et al. 2006b), due to the increased epilimnion nutrients from groundwater diffusion and lake overturn (Schettler et al. 2006b). Diatoms in this lake are highly diverse and, *Staurosira longwanensis* Rioual, Morales & Ector, has been described as a new species from material collected in this lake (Rioual et al. 2014, 2016).

Materials and methods

The Sihailongwan sediment composite profile is combined from three overlapping adjacent cores to produce a continuous sequence spanning the last 65,000 calibrated years BP (cal yr BP). The three cores were retrieved from Sihailongwan in 2001 using a high-precision Usinger corer (Parplies et al. 2008; Mingram et al. 2009, 2018). The age of the sediment core is based on varve chronology corrected with AMS ^{14}C dates together with several well-dated and widespread tephra layers which have been used as tephrochronology tie-points and age controls (Mingram et al. 2009). Details of the age-depth model were given in Mingram et al. (2018) and summarised in Fig. S1.

Seven major tephra layers and numerous micro-tephra layers have been identified in the Sihailongwan sediment sequence (Mingram et al. 2018). Five tephra layers named T1, T2, BT, T4 and AT, with thicknesses ranging from > 18 cm to micro-tephra < 1 cm have been chosen for investigation in this study. The tephra layers span across a large section of the sediment core occurring in different depths, time intervals and climatic conditions. Four of the five tephra layers are basaltic in nature and one tephra layer is rhyolitic (Table 1; Fig. S2). The five tephras can be broadly classified into three categories according to their thicknesses: very thick tephra > 15 cm (T2); thick tephra 5–15 cm (T1 and T4); micro-tephra < 1 cm (BT and AT).

To investigate the diatom and the lake's responses to the five tephras, three adjacent 1 cm samples above and below each tephra layer were selected for investigation. Additionally, samples containing the tephra layers were also analysed (Fig. S2). Higher resolution sampling was not possible because the entire sequence had already been sliced in contiguous 1-cm thick samples. A total of 39 samples were analysed for diatoms. Diatom-slide preparation largely followed Battarbee et al. (2001). 30% H_2O_2 and HCl were added to each sample (0.01 g of sediment placed in a test tube) to remove organic materials and carbonates. The tubes were then filled with distilled water and the suspensions left to settle overnight.

Table 1 Characteristics of the five tephra layers investigated in this study. The geochemical compositions and source of tephra data are from Zhao and Hall (2015), Miyairi et al. (2004), Mingram et al. (2009), Liu et al. (2009) and Zhao et al. (2017). The background climate information associated with tephra are from Stebich et al. (2007, 2009, 2015), Schettler et al. (2006a, b), Mingram et al. (2018), Zhu et al. (2021) and Parplies et al. (2008). The climate and lake-trophic-status reconstructions were based on a range of proxies including pollen, branched glycerol dialkyl glycerol tetraethers (brGDGTs), geochemical and stable isotope analyses

Tephra	Depth (cm)	Age (cal yr BP)	Thickness (cm)	Overall chemistry	Geochemical compositions				Volcanic source	Background climate and inferred lake condition
					SiO_2(wt%)	Na_2O (wt%)	K_2O (wt%)	P_2O_5 (wt%)		
Tephra 1 (T1)	112.5–119.5	2012	7	Trachybasaltic	48.25	4.81	2.88		Jinlongdingzi Volcano	Late Holocene. Slight cooling trend and slight shift in forest cover to herbaceous drought-tolerant vegetation, e.g., taiga and steppe. Shortened growing seasons
Tephra 2 (T2)	365.5–383.5	10422	15–19	Trachybasaltic	46.44	3.22	2.13	0.52	Jinlongdingzi Volcano	Early Holocene. Increased temperature, precipitation and forest cover. Vegetation shift from birch-dominated pioneer species to temperate deciduous forests. Enhanced lacustrine productivity
Basaltic microtephra (BT)	642.5	15686	~0.05	Trachybasaltic					Possibly local LVF eruption	Late glacial. Relatively cold conditions characterised with low lacustrine productivity. Coincided with Heinrich event 1

Table 1 (continued)

Tephra	Depth (cm)	Age (cal yr BP)	Thickness (cm)	Overall chemistry	Geochemical compositions				Volcanic source	Background climate and inferred lake condition
					SiO_2(wt%)	Na_2O (wt%)	K_2O (wt%)	P_2O_5 (wt%)		
Tephra 4 (T4)	1290.5–1296.5	24770	6	Trachybasaltic	49.59	5.05	2.80		Possibly local LVF eruption	Last Glacial Maximum. Low lacustrine productivity. Lake catchment likely affected by permafrost cover. Coldest conditions among 5 tephra layers. Lowered lake water level due to dryer and cooler climate. High aeolian clastic influx. Vegetation composed of steppe patches
Aira-Tn microtephra (AT)	1481.5	29618	~0.05	Rhyolitic	74.51	2.94	3.10	0.02	Aira caldera, Japan	Transition into the Last Glacial Maximum. Cold and dry climate. Low lacustrine productivity. High aeolian clastic influx

The resultant supernatant liquid was removed. Microspheres were added for the calculation of diatom concentrations (Battarbee and Kneen 1982) that were expressed in number of valves per gram of dry sediment. Lastly, the samples were pipetted onto coverslips and mounted with Naphrax® on a hotplate onto microscope slides. Diatom valves were counted under a light microscope with oil immersion at × 1000 magnification. A minimum of 500 valves were counted for each sample, except for those diatom-barren 'within-tephra' samples. Diatom species were identified mainly using Krammer and Lange-Bertalot (1986, 1988, 1991a, b) and Lange-Bertalot et al. (2017). Some regional floras from Mongolia, Korea and Russia: (Metzeltin et al. 2009; Joh 2010, 2011; 2012a, b; Lee 2011, 2012; Kulikoskiy et al. 2016) were also employed. For the "*Cyclotella comensis*" complex we follow Scheffler and Morabito (2003) and Scheffler et al. (2005) who studied the life cycle of this diatom, including populations from the type location (e.g. Lake Como, Italy), and distinguished two morphotypes *Cyclotella comensis morphotype comensis and Cyclotella comensis morphotype minima*. The latter differs from the nominal form by its smaller cell size and smoother valve surface. The population observed in the sediment sequence from Lake Sihailongwan is also composed of two morphotypes whose morphological characteristics match with those described in Scheffler and Morabito (2003). *Cyclotella comensis* has recently been transferred to the genus Pantocsekiella by Ács et al. (2016) but only the nominal form was considered. Here we erect a new combination for the morphotype *minima* that we consider as a forma, in accordance with the International Code of Botanical Nomenclature.

Pantocsekiella comensis fo. *minima* (Scheffer & Morabito) Rioual comb. nov.

Basynonym: *Cyclotella comensis* morphotype *minima* Scheffler & Morabito 2003, in Scheffler W. and Morabito G. 2003, Journal of Limnology 62: 49.

Chrysophyte cysts and their scales were counted at the same time as the diatoms but enumerated separately. However, no attempt was made to identify different cyst morphologies due to the lack of knowledge and the current difficulties in assigning chrysophyte cysts to taxonomic names (Pla et al. 2003).

Using Canoco 5.0 (ter Braak and Šmilauer 2012), detrended correspondence analysis (DCA) was first performed on a reduced dataset including diatom taxa whose abundances were ≥ 2% from all samples spanning the five tephra layers investigated. Diatoms data were square root transformed and rare taxa downweighed to reduce noise. For individual tephra, a non-metric multidimensional scaling (nMDS) analysis using Bray–Curtis similarity index was carried out for species concentrations. nMDS was chosen over other multivariate techniques because it does not take absolute distances between samples into account and only computes the relative distances between samples (Hammer et al. 2001). It also does not assume any underlying variable-environmental relationships (Hutchinson et al. 2019). This method is appropriate for this study as it is concerned with the degree of tephra-induced changes relative to the background-condition fluctuations between a small number of samples.

For diatom stratigraphical diagrams, only taxa with abundances ≥ 5% have their concentrations plotted. Species < 5% have been merged to their genus level. If the genus percentages are still < 5% after merging, they were put into 'other planktonic' or 'other benthic' depending on their habitat type. Concentrations are presented rather than relative percentage abundances since concentrations enable better comparisons between samples and visualisation of diatom-production changes, while also allowing examination of changes in assemblage structures. Two additional indices—planktonic/benthic diatom ratio (P/B) and diatom/chrysophyte-cyst ratio (D/C) are also presented in the stratigraphical diagrams. P/B ratio is calculated by dividing the total planktonic diatom concentration with the total benthic diatom concentration. Similarly, D/C ratio is calculated by dividing the total diatom concentration with the total chrysophyte-cyst concentration.

Results

Down-core variations of all samples

The DCA analysis on all samples presents an overall picture of down-core variations in background conditions (Table S1 shows the summary statistics). An axis 1 gradient of 4.09 (> 3) was obtained, suggesting

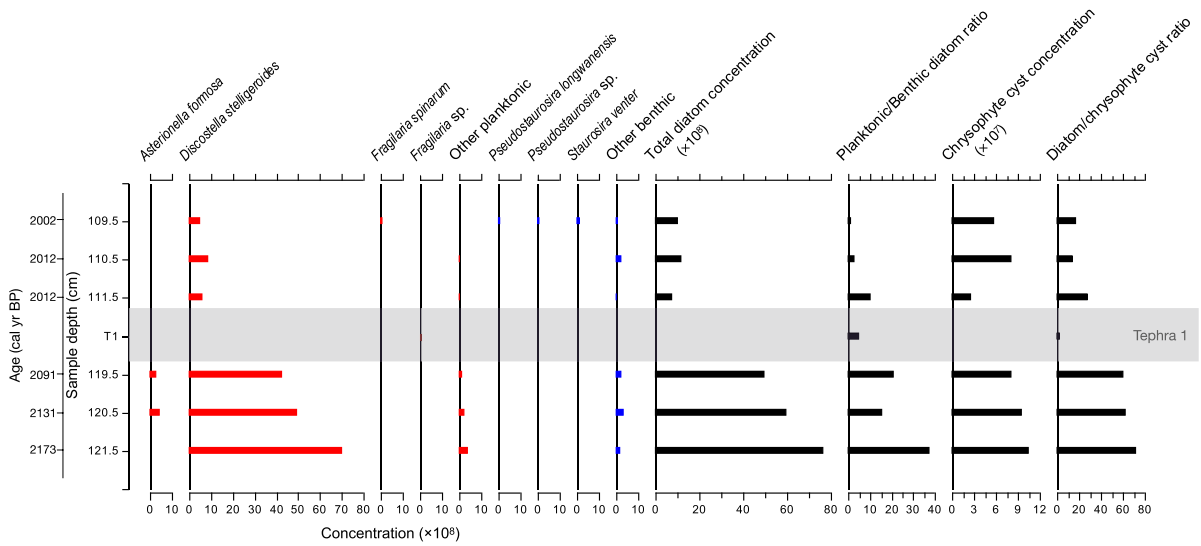

Fig. 3 Stratigraphy of diatom and chrysophyte-cyst concentrations in samples associated with T1. Planktonic and benthic diatom species are represented in red and blue, respectively

that the use of DCA was appropriate. However, the cumulative explained variation of axes 1 and 2 is only 36.2%. The DCA ordination plot indicates distinct clusterings between samples associated with different tephras (Fig. S3). 'Within-tephra' samples have not been included due to their very low diatom counts that biased their relative percentages.

Diatom and chrysophyte-cyst analysis before and after T1 (thick tephra)

Planktonic diatom species make up most of the assemblages, with *Discostella stelligeroides* (Hustedt) Houk & Klee being dominant (Fig. 3) representing ≥ 50% of the assemblages in all samples and occurring at exceptionally high concentrations before the deposition of T1. *Asterionella formosa* Hassall also occurs at relatively higher concentration compared to other taxa before T1 deposition. The most significant change after T1 deposition is the decrease (from ~ 45×10^8 to ~ 10×10^8 valves g^{-1}) in *Discostella stelligeroides* concentration. Other planktonic species such as *Asterionella formosa* also display reduced concentrations. Total diatom concentration decreases dramatically after T1 deposition from ~ 75×10^8 to ~ 10×10^8 valves g^{-1} and chrysophyte-cyst concentration decreases from ~ 8×10^7 to ~ 3×10^7 cysts g^{-1} after T1. The P/B ratio and D/C ratio decrease by almost half, which are mainly results of the *Discostella stelligeroides* concentration decrease. The nMDS on diatom concentrations indicates a large shift after T1 deposition. The degree of change within the background pre-tephra samples is negligible compared to the change between the most immediate pre- and post-tephra samples (Fig. 4).

Diatom and chrysophyte-cyst analysis before and after T2 (very thick tephra)

The planktonic species *Stephanodiscus minutulus* (Kützing) Cleve & Möller is the most abundant species before T2 deposition occurring at concentrations ~ 90–110 × 10^7 valves g^{-1} (Fig. 5). *Fragilaria gracilis* Østrup and other benthic species are also present at relatively high concentrations of ~ 20–30 × 10^7 valves g^{-1} and ~ 20–50 × 10^7 valves g^{-1}, respectively. Total diatom concentrations are ~ 15–20 × 10^8 valves g^{-1} and chrysophyte-cyst concentrations are ~ 4–8 × 10^7 cysts g^{-1}. After T2 deposition, *Stephanodiscus minutulus* decreases to almost zero immediately post-tephra, as well as *Fragilaria gracilis* and other benthic diatoms. Likewise, total diatom concentration and chrysophyte-cyst concentration decrease substantially to near zero after T2 deposition. The P/B ratio does not exhibit a change immediately after T2, but an

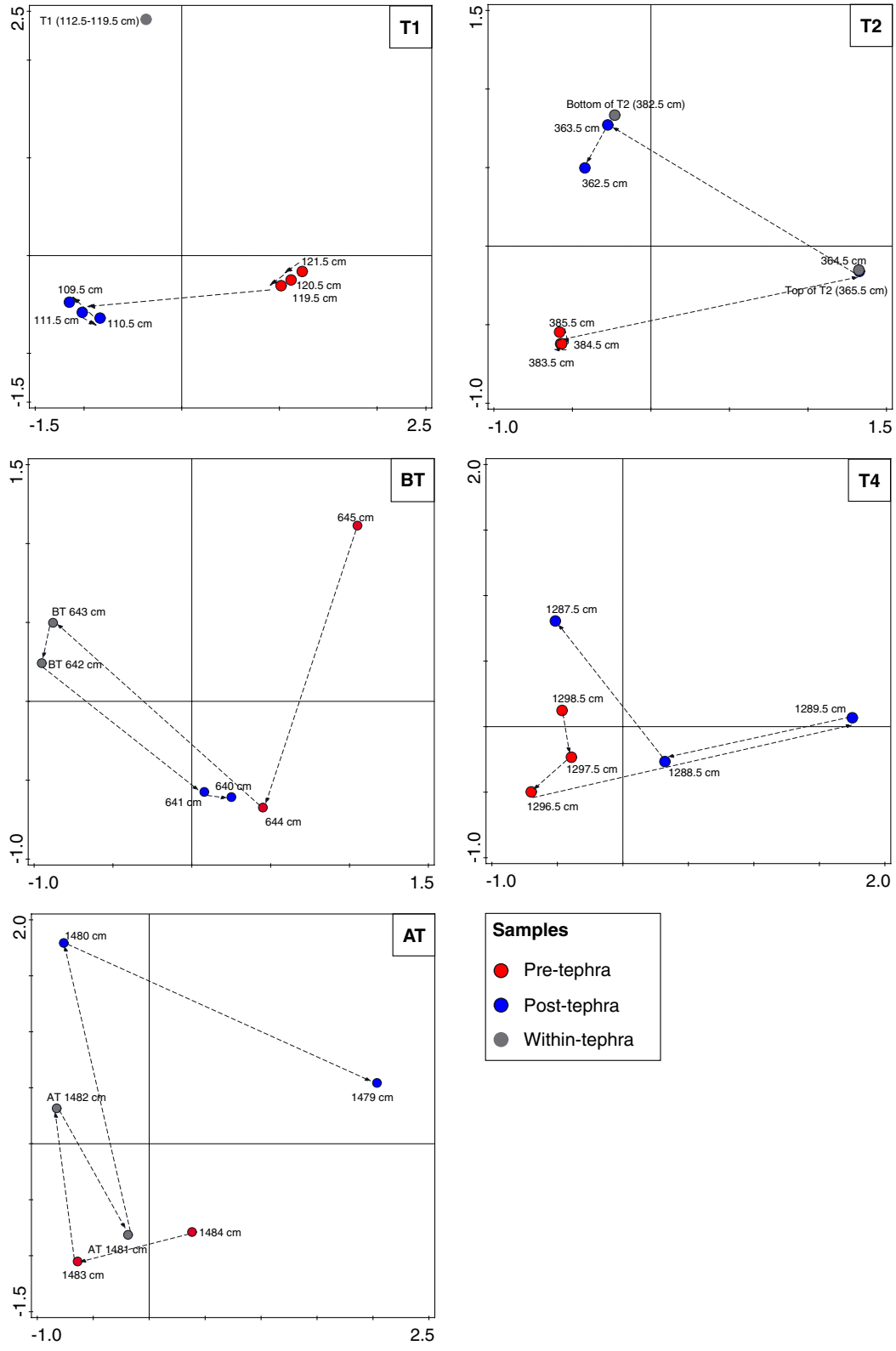
T1
T1 (112.5-119.5 cm)
121.5 cm
120.5 cm
119.5 cm
109.5 cm
111.5 cm
110.5 cm
2.5
-1.5
-1.5
2.5
T2
Bottom of T2 (382.5 cm)
363.5 cm
362.5 cm
364.5 cm
Top of T2 (365.5 cm)
385.5 cm
384.5 cm
383.5 cm
1.5
-1.0
-1.0
1.5
BT
645 cm
BT 643 cm
BT 642 cm
640 cm
641 cm
644 cm
1.5
-1.0
-1.0
1.5
T4
1287.5 cm
1298.5 cm
1289.5 cm
1297.5 cm
1288.5 cm
1296.5 cm
2.0
-1.0
-1.0
2.0
AT
1480 cm
1479 cm
AT 1482 cm
1484 cm
AT 1481 cm
1483 cm
2.0
-1.5
-1.0
2.5
Samples
Pre-tephra
Post-tephra
Within-tephra

◂**Fig. 4** nMDS plots on diatom concentrations in samples associated with T1, T2, BT, T4 and AT. The directions of change related to a tephra have been indicated by arrows

increase of ~ 40 is observed in the subsequent sample 363.5–364.5 cm. nMDS of diatom concentrations in samples associated with T2 shows a relatively large degree of change that can be attributed to T2 deposition. However, a large shift can also be seen between two post-tephra samples (364.5 cm and 363.5 cm; Fig. 4).

Diatom and chrysophyte-cyst analysis before and after BT (micro-tephra)

In samples before micro-tephra BT, large fluctuations are already observed in the more abundant taxa such as *Pantocsekiella comensis* f. *minima* and *Discostella stelligeroides.* This is also true for total diatom concentrations and chrysophyte-cyst concentrations. Upon BT deposition, an increase in the concentrations of *Discostella stelligeroides* is observed in the two samples where BT is located (642–643 cm and 643–644 cm; note that for micro-tephras there are no within-tephra samples, micro-tephras are contained in between two non-tephra samples; Fig. 6). For other taxa such as *Pantocsekiella comensis* fo. *minima*, *Pantocsekiella rossii* (H.Håkansson) K.T.Kiss & E.Ács and *Stephanocostis chantaicus* Genkal & Kuzmina, variable increase and decrease in concentrations are observed in the stratigraphical diagrams but without distinct and coherent patterns. Total diatom concentration increases by ~ 2×10^8 valves g^{-1} upon deposition of BT. However, the same magnitude of change is also observed in samples before BT deposition. The P/B ratio increases in general throughout this period. Chrysophyte cysts show a slight decrease, although their concentration seems to be stable in samples adjacent to the micro-tephra layer. The D/C ratio increases by almost 2/3 after BT deposition from ~ 15 to ~ 25, then decreases (Fig. 6). The nMDS plot shows that the immediate samples associated with BT (643 cm and 642 cm) exhibit a very small degree of variation compared to other non-tephra samples (Fig. 4).

Diatom and chrysophyte-cyst analysis before and after T4 (thick tephra)

Prior to T4 deposition, the diatom assemblage is characterised by two dominant planktonic species *Pantocsekiella comensis* f. *minima* and *Pantocsekiella rossii* as well as a diverse range of benthic species. *Pantocsekiella comensis* f. *minima* occurs at concentration of ~ 20×10^6 valves g^{-1} and *Pantocsekiella rossii* occurs at concentration of ~ 20–30 $\times 10^6$ valves g^{-1}. Total diatom concentration is relatively constant before tephra deposition at ~ 15×10^7 valves g^{-1}. Chrysophyte-cyst concentration is already in a decreasing trend. The most distinct changes after

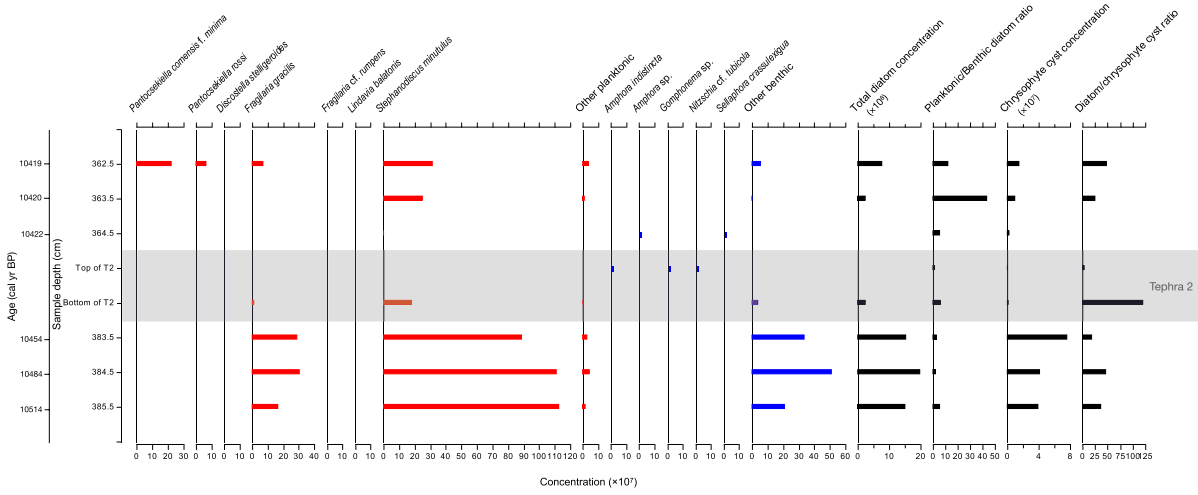

Fig. 5 Stratigraphy of diatom and chrysophyte-cyst concentrations in samples associated with T2. Planktonic and benthic diatom species are represented in red and blue, respectively

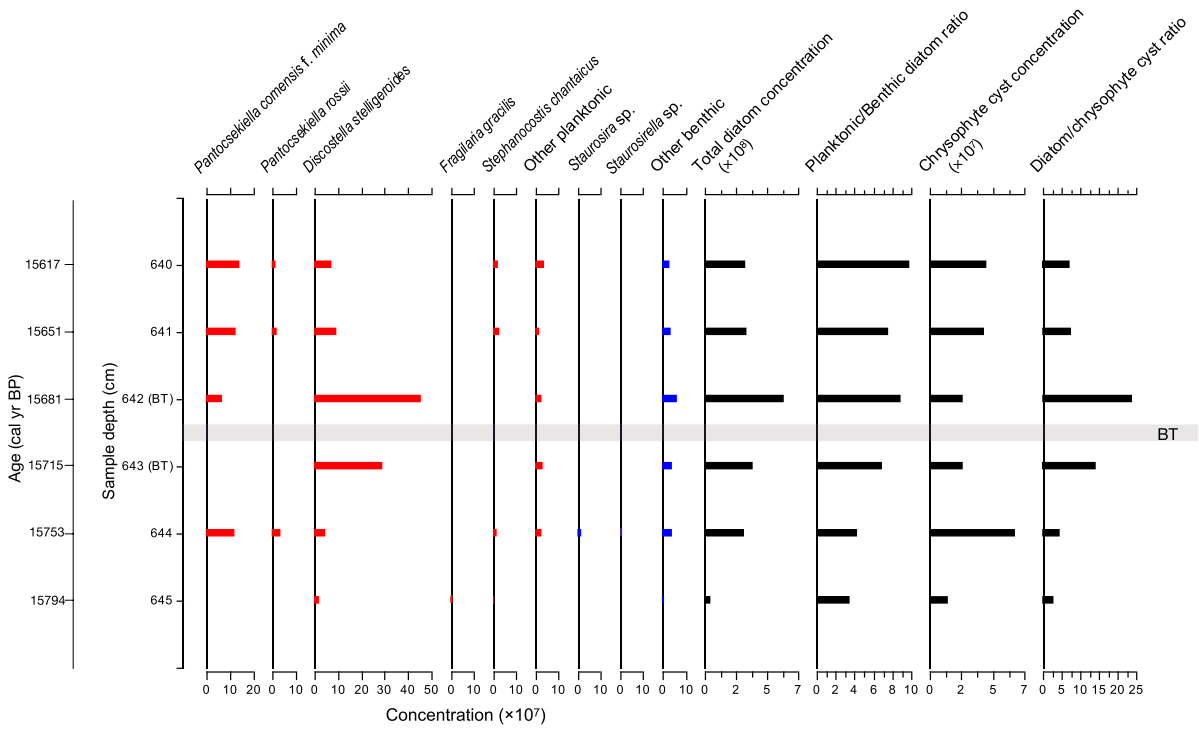

Fig. 6 Stratigraphy of diatom and chrysophyte-cyst concentrations in samples associated with BT. Planktonic and benthic diatom species are represented in red and blue, respectively

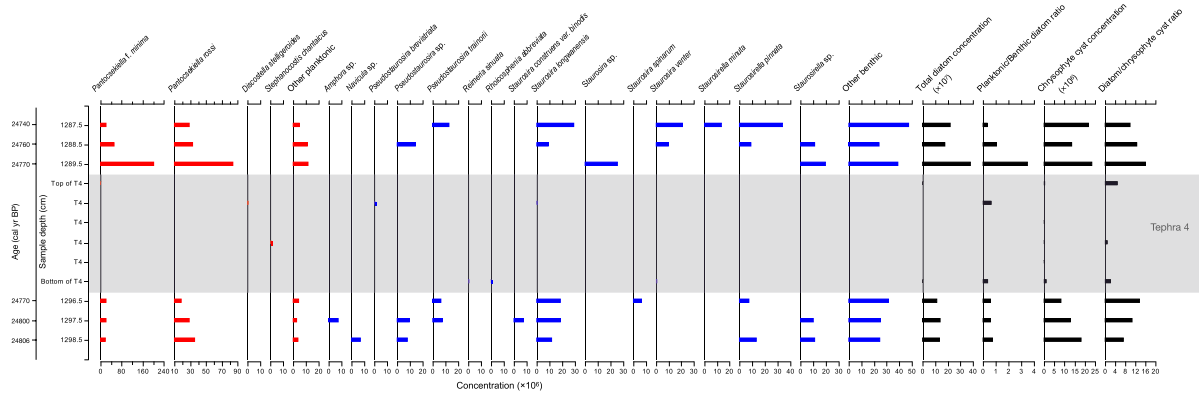

Fig. 7 Stratigraphy of diatom and chrysophyte-cyst concentrations in samples associated with T4. Planktonic and benthic diatom species are represented in red and blue, respectively

T4 are the clear increase in *Pantocsekiella comensis* f. *minima* and *Pantocsekiella rossii* concentrations (Fig. 7). *Pantocsekiella comensis* f. *minima* increases to ~ 200×10^6 valves g^{-1} post-tephra, with a subsequent decrease. Similarly, *Pantocsekiella rossii* increases to ~ 80×10^6 valves g^{-1} post-tephra, then also experiences a subsequent decrease. After T4, benthic species such as *Staurosira longwanensis*, *Staurosira venter* (Ehrenberg) Cleve & J.D.Möller and *Staurosirella pinnata* (Ehrenberg) D.M. Williams & Round increase in their dominance not immediately after tephra deposition, but in the following samples. Total diatom concentration increases in the immediate post-tephra sample (1289.5–1290.5 cm)

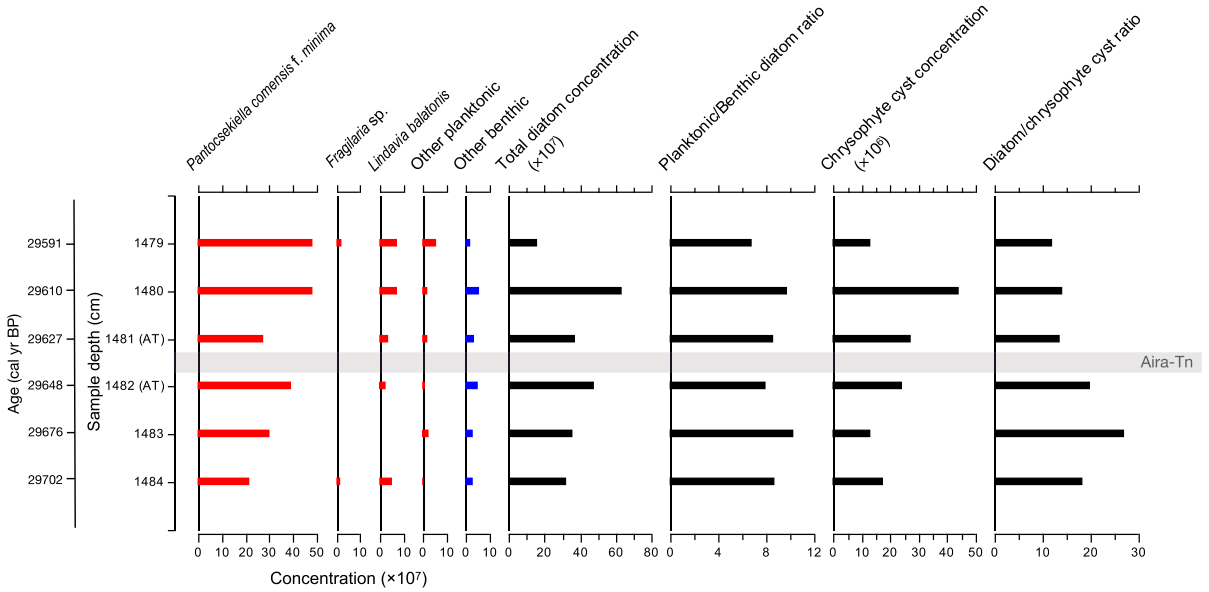

Fig. 8 Stratigraphy of diatom and chrysophyte-cyst concentrations in samples associated with AT. Planktonic and benthic diatom species are represented in red and blue, respectively

from ~ 1.2×10^8 to ~ 4×10^8 valves g^{-1}, then decreases to ~ 2×10^8 valves g^{-1}. The P/B ratio also increases after T4 deposition by a value of ~ 3, then decreases to values like those in pre-tephra samples. Chrysophyte cysts increase in concentration after T4 deposition. The D/C ratio increases slightly from ~ 14 to ~ 17. nMDS on diatom concentrations shows that the strongest variation is between the samples immediately pre- and post-tephra as represented by the longest relative distance (Fig. 4).

Diatom and chrysophyte-cyst analysis before and after AT (micro-tephra)

Pantocsekiella comensis f. *minima* dominates in all samples associated with AT, together with relatively high concentrations of *Lindavia balatonis* (Pantocsek) Nakov, Guillory, Julius, Theriot & Alverson (Fig. 8). Before the deposition of AT, *Pantocsekiella comensis* f. *minima* had already increased from ~ 20×10^7 to ~ 40×10^7 valves g^{-1}. The total diatom concentration is ~ 35–40×10^7 valves g^{-1} and the chrysophyte-cyst concentration is ~ 15–25×10^6 cysts g^{-1}. Chrysophyte-cyst concentration is variable even before AT. *Pantocsekiella comensis* f. *minima* decreases immediately after tephra deposition to ~ 30×10^7 valves g^{-1} and increases again to ~ 50×10^7 valves g^{-1} in this period (29,697–29,799 cal yr BP). In contrast, other less dominant species such as *Fragilaria* sp. and *Lindavia balatonis* exhibited very minor variations with no prominent patterns. Fluctuations in total diatom concentration are observed, however, it is uncertain whether changes in total diatom concentration relate to AT deposition. A small decreasing trend can be seen in the P/B ratio, but likewise changes cannot be linked to the tephra unambiguously. Similarly, the D/C ratio shows a certain level of fluctuation, however, any linkage to AT deposition is ambiguous. nMDS on diatom concentrations suggests small or similar degrees of change in samples directly associated with AT (1482 cm and 1481 cm) to those from background samples (Fig. 4).

Discussion

Overall diatom trends from the Last Glacial Maximum (LGM) to the Holocene

The five tephra layers were deposited in different time intervals characterised by different climatic conditions (Table 1; Fig. 9), which is emphasised by the DCA plot for all diatom samples (Fig. S3) illustrating

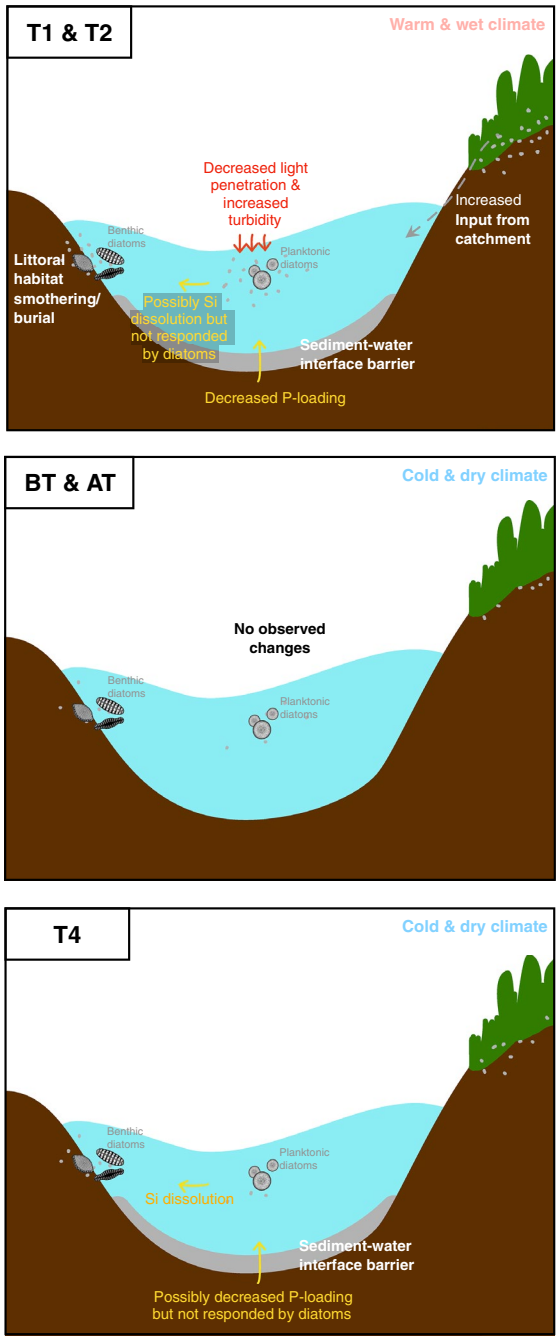

Fig. 9 Schematic diagrams showing physical and biochemical lacustrine responses to five different tephra depositions in Lake Sihailongwan under varying background conditions

distinct clustering of samples associated with each tephra.

The oldest tephra analysed in this study, AT (28,037 cal yr BP) corresponds with the onset of the LGM and likely represented similar but not as severe climate conditions to T4 (which is the same minerogenic clastic varve type; Mingram et al. 2018; Zhu et al. 2021). This is manifested by the low diatom concentrations and *Pantocsekiella comensis* f. *minima* being dominant (Fig. 8).

T4 (24,770 cal yr BP) was deposited during the LGM, most probably under the coldest conditions of the five tephras (Mingram et al. 2018; Zhu et al. 2021). Similar to BT (15,686 cal yr BP), this period shows low overall diatom production and was mainly dominated by *Pantocsekiella comensis* f. *minima* and *Pantocsekiella rossii* but not *Discostella stelligeroides* (Fig. 7). This suggests even more oligotrophic lake conditions and low groundwater-nutrient input as well as terrestrial biogenic productivity.

The overall diatom concentration at the time of BT deposition (15,686 cal yr BP) was lower compared to T1 and T2, suggesting lower lake productivity under cooler and possibly drier conditions (Stebich et al. 2007, 2009; Parplies et al. 2008). Relatively high abundances of *Pantocsekiella* and *Discostella* species (Fig. 6) are seen between 15,689 and 15,816 cal yr BP and *Pantocsekiella comensis* f. *minima* and *Pantocsekiella rossii* both occur under low productivity conditions (Scheffler and Morabito 2003; Saros and Anderson 2015; Ossyssek et al. 2020). *Discostella stelligeroides* is found in oligotrophic to mesotrophic conditions (Houk et al. 2010).

T2 (10,422 cal yr BP) occurred shortly after the onset of the Holocene (abrupt warming; Stebich et al. 2007, 2015). This period is dominated by *Stephanodiscus minutulus* (Fig. 5), a species with high P requirements (Van Dam et al. 1994; Interlandi et al. 1999; Reavie et al. 2000). Similar to T1, this also indicates a period of elevated lake nutrients from groundwater and terrestrial inputs.

T1 (2012 cal yr BP) was deposited in a climate characterised by relatively warmer temperature and higher precipitation as inferred from pollen analysis (Stebich et al. 2007, 2015). This is consistent with the very high overall diatom concentrations, implying high diatom productivity and high nutrient status in Sihailongwan during this period. There was likely a high dissolved nutrient supply due to enhanced

groundwater discharge and high terrestrial productivity (Schettler et al. 2006a).

Aquatic responses to different tephra thickness

Consequences of very thick tephra deposition (T2–15–19 cm thick)

For the very thick tephra T2, diatom concentrations show significant tephra-related changes relative to background fluctuations as indicated by the nMDS plot (Fig. 4). The sample immediately post-T2 had a significantly different diatom concentration from background samples as well as the two following samples with the immediately post-T2 sample containing negligible diatom concentrations resembling those 'within-tephra' samples. The decrease in diatom production post-T2 is manifested across all species but especially by *Stephanodiscus minutulus*, the dominant species in background samples (> 50%). *Stephanodiscus minutulus* is a eutrophic species with high P requirements (Interlandi et al. 1999; Reavie et al. 2000). This may suggest a decrease of P in Sihailongwan after T2 deposition due to a lake-bottom-tephra barrier limiting P-loading (Fig. 9; Telford et al. 2004). T2 has a thickness of 15–19 cm and was deposited in the early Holocene, a period of high temperature, precipitation and terrestrial productivity. Nutrient levels within the lake were probably relatively high. Therefore, a decrease in P input would have had a profound effect on diatom productivity, especially in a volcanic setting such as that of Sihailongwan where nutrient conditions are highly dependent on groundwater influx (Telford et al. 2004; Schettler et al. 2006a). This is a highly probable scenario considering the thickness of T2 (15–19 cm), which would have likely covered the entire lake bottom. Nevertheless, the effect of reduced P seems to be short-lived. Overall diatom concentrations, especially planktonic diatoms (mainly *Stephanodiscus minutulus*) started to increase in the next consecutive sample after the immediate post-tephra sample. In their study on the Holocene sequence of Sihailongwan, based on geochemical proxy indicators, Schettler et al. (2006a) recorded a rise in $bSiO_2$ flux rate after T2 and related this to increased diatom productivity due to the enhanced inflow of nutrients from eroded pumice tuff in the lake catchment. Our results imply that the release of nutrients from catchment pumice did not occur immediately after T2 but only started after 3–10 years.

It is assumed that T2 had a major burial impact owing to its thickness, destroying the diatom communities to an extent where the lake conditions turned to a state quasi-devoid of life. The sequential occurrences of *Amphora, Gomphonema, Nitzschia* and *Sellaphora* species after tephra deposition indicate the early recolonisation of diatoms in a harsh environment, as these benthic species were not present or only present in small percentages before the deposition of T2. In particular, *Nitzschia* species are highly motile and can avoid burial in the sediments (Lowe 2003; Kociolek 2011; Solak et al. 2019). Similarly, *Sellaphora* species also have an epipelic habitat and wide environmental tolerances (Van Dam et al. 1994; Wetzel et al. 2015).

Low concentrations of *Stephanodiscus minutulus* were found in the bottom-most 'within-tephra' sample, while several benthic species that were not present in any other samples were found in the top-most 'within-tephra' sample. The poor sorting of the material suggests that after the initial airfall a slump may have occurred with T2, in-washing tephra and sediments from the catchment and introducing benthic species into the lake centre where the core was taken. As such, T2 is probably composed of a mixture of airborne tephra material and in-washed/slump material. Another possible explanation is that the tephra boundaries were not determined accurately when the core was sliced into 1-cm thick samples. Accordingly, the species found in the top-most 'within-tephra' sample could represent early lake responses to tephra deposition, but they have been allocated into 'within-tephra' due to the ambiguous tephra boundaries (Payne and Egan 2019).

Chrysophyte-cyst changes are in concordance with diatom changes. The decline in chrysophyte-cyst concentration after T2 deposition suggests a decline in lake nutrients, especially Si (Fig. 5; Douglas and Smol 1995; Pla and Anderson 2005). Chrysophyte cysts are highly silicified and therefore have high Si requirements. Today, Si is also a limiting nutrient in Sihailongwan and it is supplied together with P through groundwater inflow (Schettler et al. 2006a). Thus, it is likely that the lake-bottom-tephra barrier also impeded Si diffusion into the water column.

Consequences of thick tephra depositions (T1-7 cm thick and T4-6 cm thick)

T1 and T4 have a similar thickness of 7 and 6 cm, respectively, however they were deposited at different times under different local climate regimes (Table 1). T1 was deposited in the late Holocene with similar conditions to T2 (early Holocene). T4 on the contrary was deposited during the LGM when climate conditions were the most unfavourable for diatom growth with low precipitation, temperature and groundwater-nutrient flux (Stebich et al. 2007). Despite the similarity in tephra thickness, the lake responded to these tephra depositions in contrasting ways due to differences in background climate and lake conditions.

Overall diatom production decreased after T1 deposition, likely due to the presence of a tephra barrier on the water–sediment interface, preventing P-loading from groundwater into the lake through a mechanism similar to that which occurred with the very thick tephra, T2 (Fig. 9). Although Barker et al. (2000) suggested that only tephra layers with thicknesses > 10 cm can significantly limit P diffusion, T1 was only 7 cm in thickness but still had an effect. The eutrophic background conditions probably exacerbated diatoms' responses to decreased P and furthermore, T1 was a basaltic tephra with very low SiO_2 content. A decline in concentration was observed mainly for planktonic species as suggested by the decline in P/B ratio (Fig. 3). This was especially so for *Discostella stelligeroides* which is a species with small cell size and fast growth rate that can respond quickly to nutrient enrichment (Saros and Anderson 2015). This may also be true for its response to nutrient depletion. *Asterionella formosa*, an eutrophic species (Lund 1950), also shows the same decreasing trend. Eutrophic species have narrower environmental tolerances than oligo-mesotrophic species, therefore even small fluctuations in the nutrient status can induce large alterations in their population abundances (Passy 2008). T1 possibly also had a burial effect on littoral habitats as suggested by an increase in 'deep benthic' taxa that can be found in epipsammic habitats (for example small *Staurosirella, Staurosira* and *Pseudostaurosira*) after T1 deposition. However, these taxa do not appear in the sample immediately post-tephra, the immediate onset of T1 probably created conditions too harsh for an epipsammic assemblage to develop. As time passed, harsh burial conditions eased which created habitats suitable for these species. These observations are almost identical to those reported by Egan (2016) from a lake in Washington, USA, where she also attributed them to habitat alterations and new species colonisation. Another potential impact of T1 was sustained water-column turbidity (Fig. 9). *Discostella stelligeroides* has very high light requirements for photosynthesis (Saros and Anderson 2015), and its concentration remained relatively low for > 30 years after T1. Although the effect of light limitation is believed to only last for days (Barker et al. 2000), we cannot rule out the possibility of prolonged in-wash of fine tephra materials from the lake catchment (Christensen 2011). Since Sihailongwan was in proximity to the Jinlongdingzi Volcano (the source of T1), tephra was probably deposited in huge quantities on the catchment. As a consequence of the wet and warm climate of this period, substantial amounts of terrestrial tephra could have been weathered and washed into the lake for years after the eruption. The spring–summer peak precipitation in this region also coincides with the intra-annual diatom bloom (Schettler et al. 2006b), introducing water turbidity from catchment erosion that could have profoundly limited *Discostella stelligeroides* growth.

In contrast to T1, an abrupt increase in overall diatom concentration was observed immediately after T4 deposition, especially in planktonic species as indicated by the increase in P/B ratio (Fig. 7). Major increases in concentration were seen in *Pantocsekiella comensis* f. *minima* and *Pantocsekiella rossii.* The enhancement in the concentrations of small centric planktonic diatom species after deposition of T4 possibly indicates an increase of lake nutrients. This is because smaller-sized diatoms have faster growth rates and lower nutrient-use efficiency, therefore their populations tend to increase under higher nutrient availability (Saros and Anderson 2015; Wentzky et al. 2020). While both *Pantocsekiella* species showed concentration increases, *Pantocsekiella comensis* f. *minima* responded more abruptly due to its smaller cell size, it is also referred to as an 'opportunistic' species (Scheffler and Morabito 2003; Ossyssek et al. 2020). Generally, *Pantocsekiella* species are believed to be good at taking advantage of an input of Si to develop large populations in oligotrophic lakes. Therefore, the increase in *Pantocsekiella* potentially indicates that the lake SiO_2 was elevated through the

dissolution of tephra particles in the water column. T4 was deposited during the LGM when the climate conditions were the most unfavourable for diatoms to develop, with low precipitation, temperature and groundwater-nutrient flux. The nutrient levels in Sihailongwan were possibly very low, thus even small increases in lake Si content could trigger ecosystem change. Additionally, if T4 had imposed a barrier effect for nutrient diffusion into the water column, this effect was not significant as the nutrient input was already low; the lake would not respond dramatically to any further decreases. The inference that the dissolution of SiO_2 from tephra caused the increased diatom concentrations observed in Sihailongwan seems more probable.

Chrysophyte-cyst changes broadly echo the diatom-inferred changes both for T1 and T4. The D/C ratio decreased after T1 (Fig. 3). The D/C ratio can be used as an inference for lake-trophic change, where a decrease in this ratio often reflects decrease in nutrients (Douglas and Smol 1995; Pla and Anderson 2005). This is because chrysophytes tend to thrive more in oligotrophic conditions due to their high capabilities for nutrient sequestering and storage (Lotter et al. 1998). On the contrary, they tend to get outcompeted by diatoms in eutrophic conditions owing to their lower growth rate (Duff et al. 1997). By contrast, increased chrysophyte-cyst concentrations are seen after T4 deposition and the D/C ratio also decreased (Fig. 7). Chrysophyte cysts are highly silicified, therefore increasing Si would boost their growth. Furthermore, chrysophytes could be more sensitive to nutrient changes than diatoms (Lotter et al. 1998), meaning that they could take advantage of even small elevations in Si introduced by a basaltic tephra.

Micro-tephras (BT – 0.05 cm thick and AT – 0.05 cm thick)

No significant diatom or chrysophyte-inferred changes can be associated with the two micro-tephras BT and AT (Fig. 9). From the nMDS plots of diatom concentrations in samples associated with BT and AT, the background samples show large fluctuations and the degree of change between background samples was as large if not larger than the change between the pre- and post-tephra samples. This is also illustrated by overall diatom concentration, P/B ratio and chrysophyte-cyst concentration (Figs. 6 and 7).

BT for example, exhibited slight rises in overall diatom concentration (Fig. 6), especially by *Discostella stelligeroides* and some benthic diatoms after deposition. However, these concentrations were already increasing before the deposition of BT. BT may have been too small to induce any identifiable chemical or physical alterations of the lake system (Telford et al. 2004).

Another plausible explanation for the inability to attribute changes to tephras is the low confidence about which of the samples analysed for diatoms actually contain the BT layer and whether the immediately pre- and post-tephra samples truly constitute the correct pre- and post-tephra diatom assemblages. Since the thickness of BT was < 1 cm, thinner than the sample resolution, it is impossible to distinguish the potential immediate effect of BT as both the pre- and post-tephra diatom assemblages are all contained within one 1-cm thick sample. Additionally, the photograph of the core shows that there was a slight bending in the laminae, an artefact due to the coring/extruding (Fig. S2), further complicating sample slicing.

Impact durations and recovery

Apart from the two micro-tephras (BT and AT), none of the other tephras exhibited complete recovery back to their background conditions through the intervals investigated in this study. After T4, there was a tendency of shifting towards the background state, but diatom assemblages never returned completely back to their initial composition (Fig. 4). There are two possible explanations for this. First, the tephra (especially the very thick ones) likely caused permanent/long-term alterations of the lake ontogeny (Telford et al. 2004). This could especially be the case for small maar lakes like Sihailongwan with simple hydrogeology. Lake-system equilibriums can be shifted easily into new equilibrium states by disturbances, resulting in chronic ecosystem change (Barker et al. 2000). Another plausible explanation for the lack of recovery could be the ongoing climate changes experienced at Sihailongwan. As the tephras were altering the lake system, extraneous changes in climate and catchment conditions were also imposing influences on the lake conditions (Lotter et al. 1995;

de Klerk et al. 2008). Accordingly, any recovery signals would simply be confounded and concealed.

Limitations and implications for future tephropalaeoecological studies

While this study demonstrated the potentials of using palaeolimnology and palaeocology as methods of examining the impacts of past volcanic eruptions, major limitations were also revealed. This section outlines areas of possible improvements and some proposed principles that could inform future tephropalaeocological research:

(1) High sampling-resolution (ideally with an annual resolution). This was not possible in this study as the core had been pre-sampled at 1 cm intervals, each comprising ~ 30–40 years of sediment deposition. High sampling-resolution helps to distinguish volcanic-induced changes from background environmental fluctuations. Additionally, this would allow the capture of more subtle, complex and short-lived impacts arising from transient volcanic events, which could have been overlooked by lower sampling resolutions.
(2) Examination of species flux. This study presented diatom-species concentration instead of species-flux rate due to the lower reliability of the age controls around tephra layers (poor quality of the laminations causing larger counting errors) that prevented the calculation of sediment-accumulation rates that are necessary to compute diatom fluxes. Species flux is potentially more robust in illustrating changes in diatom assemblages as it takes into account differences in sedimentation rates.
(3) Accurate sampling of tephra horizons and 'true' pre- and post-tephra layers from the core. One major concern of this study was the inaccuracy in attributing which samples included the tephra boundaries due to the low sampling resolution that was adopted when the core was sliced. Diatoms were observed in some within-tephra samples while some non-tephra samples appeared to be diatom-barren. It is not sufficient to determine horizons based on chronology alone (Payne and Egan 2019), one needs to incorporate other examinations such as changes in stratigraphic profile and sediment physio-geochemistry in order to accurately determine different layers. Future studies would need to pay particular attention to the sampling accuracies regarding tephra layers when slicing the core into individual samples.
(4) Use of statistical analysis. Many studies do not use any statistical tests and simply look at stratigraphy to deduce the volcanic impact. Here nMDS analysis served as a useful tool to help inform whether changes in diatom assemblages could be attributed to tephra depositions or not. Such statistical analysis provides a more objective means of data interpretation (Payne and Egan 2019).

Conclusions

This study investigated the impacts of five tephras on Sihailongwan in northeast China during the past 30,000 years, through the changes in diatoms and chrysophyte cysts observed in the sediment sequence. Not all tephras induced significant shifts in the diatom communities. The two micro-tephra layers (BT and AT) did not cause significant change probably because not enough tephra material was deposited to induce lake-system alterations. The apparent lack of diatom response may also be due to the coarse sampling resolution. The effect of these two tephra layers could potentially be very short-lived (much shorter than the sampling resolution), therefore any changes in the lake system detected by diatoms were smoothed out. Conversely, the other three thicker tephras (T1, T2 and T4) showed significant pre- and post-tephra changes.

Diatom data from T1 and T2 showed significant declines in overall concentrations, signalling a decline in P concentrations, possibly from the presence of a lake-bottom-tephra barrier preventing P-loading. T4 on the other hand, showed a slight increase in diatom concentrations, indicating elevated Si concentrations. Under different background climates, diatoms and the lake responded distinctly. T1 and T2 were deposited in relatively warm and eutrophic conditions, whereas T4 was deposited during the LGM when cold climatic conditions prevailed, and the lake was oligotrophic, emphasising the importance of the background conditions in governing the lake's responses to tephra depositions.

Chrysophyte cysts and scales, although not investigated comprehensively due to methodological and taxonomic limitations, largely echoed the same signals presented by diatoms. This indicates their potential application in complementing other proxies in palaeo-reconstructions (Pla et al. 2003). Chrysophytes, like diatoms, are widely found in diverse communities in many lakes. Future research should focus on developing methods to classify chrysophyte cysts and scales to utilise this proxy to its full potential (Duff et al. 1997).

In terms of lake-system recovery from tephra disturbances, none of the three tephra layers (T1, T2 and T4) which exhibited significant tephra-induced diatom-community changes showed a complete recovery back to the background state. Tephra deposition had likely caused long-term alterations on lake ontogeny, shifting the lake system to new equilibria.

Acknowledgements We thank Prof. Guoqiang Chu and Dr. Luo Wang for their comments on tephras and diatoms, respectively, and Prof. Anson Mackay for his advice on multivariate statistical analyses. We also thank the three anonymous reviewers and the editor (Prof. Guangjie Chen) for their constructive comments on the earlier version of the manuscript.

Author contribution YD, PR and VJ wrote the manuscript. YD performed the diatom analysis, the statistical analyses and prepared all figures and tables. JM and CS provided information on the varve-based chronological model and on the tephra deposits investigated. All authors reviewed the manuscript.

Funding Patrick Rioual is currently supported by the Strategic Priority Research Program of the Chinese Academy of Sciences (grant number XDB26000000). Other authors received no specific grant from any funding agency in the public, commercial, or not-for-profit sectors.

Declarations

Conflict of interest Authors have no competing interests as defined by Springer, or other interests that might be perceived to influence the results and/or discussion reported in this paper.

References

Abella S (1988) The effect of the Mt. Mazama ashfall on the planktonic diatom community of Lake Washington. Limnol Oceanogr 33:1376–1385

Ács E, Ari E, Duleba M, Dressler M, Genkal SI, Jakó E, Rimet F, Ector L, Kiss KT (2016) *Pantocsekiella*, a new centric diatom genus based on morphological and genetic studies. Fottea 16(1):56–78

Adam DP, Mahood AD (1981) Chrysophyte cysts as potential environmental indicators. GSA Bull 92:839–844

Arnalds O (2013) The influence of volcanic tephra (ash) on ecosystems. Adv Agron 121:331–380

Ayris PM, Delmelle P (2012) The immediate environmental effects of tephra emission. Bull Volcanol 74:1905–1936

Barker P, Telford R, Merdaci O, Williamson D, Taieb M, Vincens A, Gilbert E (2000) The sensitivity of a Tanzanian crater lake to catastrophic tephra input and four millennia of climate change. Holocene 10:303–310

Battarbee RW, Jones V, Flower R, Cameron N, Bennion H (2001) Diatoms. In Smol JP, Birks HJB, Last WM (eds) Tracking Environmental Change Using Lake Sediments. Volume3: Terrestrial, Algal, and Siliceous Indicators. Kluwer Academic Publishers, Dordrecht, The Netherlands, pp 155–202

Battarbee RW, Kneen MJ (1982) The use of electronically counted microspheres in absolute diatom analysis. Limnol Oceanogr 27:184–188

ter Braak CJF, Šmilauer P (2012) Canoco reference manual and user's guide: software for ordination, version 5.0. Ithaca, Microcomputer Power

Burwell IR (2003) The responses of diatoms to the influx of tephra into lacustrine environments. MSc Thesis, University of Canterbury

Christensen CL (2011) Multi-proxy responses of Icelandic lakes to Holocene tephra perturbations. MSc Thesis, University of Colorado

Chu G, Liu J, Schettler G, Li J, Sun Q, Gu Z, Lu H, Liu Q, Liu T (2005) Sediment fluxes and varve formation in Sihailongwan, a maar lake from northeastern China. J Paleolimnol 34:311–324

de Klerk P, Janke W, Kühn P, Theuerkauf M (2008) Environmental impact of the Laacher See eruption at a large distance from the volcano: integrated palaeoecological studies from Vorpommern (NE Germany). Palaeogeogr Palaeoclimatol Palaeoeco 270:196–214

Douglas MS, Smol JP (1995) Paleolimnological significance of observed distribution patterns of chrysophyte cysts in arctic pond environments. J Paleolimnol 13:79–83

Duan Y, Zhao D, Zhang X, Xia S, Liu Z, Wang F, Li L (2009) Seismic structure and origin of active intraplate volcanoes in Northeast Asia. Tectonophysics 470:257–266

Duff KE, Zeeb BA, Smol JP (1997) Chrysophyte cyst biogeographical and ecological distributions: a synthesis. J Biogeogr 24:791–812

Eastwood WJ, Tibby J, Roberts N, Birks HJB, Lamb HF (2002) The environmental impact of the Minoan eruption of Santorini (Thera): statistical analysis of palaeoecological data from Golbisar, southwest Turkey. Holocene 12:431–444

Egan J, Allott THE, Blackford JJ (2018) Diatom-inferred aquatic impacts of the mid-Holocene eruption of Mount Mazama, Oregon, USA. Quat Res 91:163–178

Egan J (2016) Impact and significance of the deposition from Mount Mazama and Holocene climate variability in the Pacific Northwest USA. PhD Thesis, University of Manchester

Frank U (2007) Rock magnetic studies on sediments from Erlongwan maar lake, Long Gang Volcanic Field, Jilin province, NE China. Geophys J Int 168:13–26

Hammer Ø, Harper DAT, Ryan PD (2001) PAST: paleontological statistics software package for education and data analysis. Palaeontol Electron 4:1–9

Hardardóttir J, Geirsdóttir A, Thórdarson T (2001) Tephra layers in a sediment core from Lake Hestvatn, southern Iceland: implications for evaluating sedimentation processes and environmental impacts on a lacustrine system caused by tephra fall deposits in the surrounding watershed. Spec Publs Int Ass Sediment 30:225–246

Harper MA, Howorth R, Mcleod M (1986) Late Holocene diatoms in Lake Poukawa: effects of airfall tephra and changes in depth. N Z J Mar Freshwater Res 20:107–118

Hickman M, Reasoner MA (1994) Diatom responses to late Quaternary vegetation and climate change, and to deposition of two tephras in an alpine and a sub-alpine lake in Yoho National Park, British Columbia. J Paleolimnol 11:73–188

Houk V, Klee R, Tanaka H (2010) Atlas of freshwater centric diatoms with a brief key and descriptions Part III. Stephanodiscaceae A. *Cyclotella*, *Tertiarus*, *Discostella*. Fottea 10:1–498

Hutchinson SJ, Hamilton PB, Patterson RT, Galloway JM, Nasser NA, Spence C, Falck H (2019) Diatom ecological response to deposition of the 833–850 CE White River Ash (east lobe) ashfall in a small subarctic Canadian lake. PeerJ 7:e6269

Interlandi SJ, Kilham SS, Theriot EC (1999) Responses of phytoplankton to varied resource availability in large lakes of the Greater Yellowstone Ecosystem. Limnol Oceanogr 44:668–682

Joh G (2010) Algal flora of Korea. Volume 3, number 1. Chrysophyta: Bacillariophyceae: Centrales. Freshwater diatoms I. Incheon, National Institute of Biological Resources

Joh G (2011) Algal flora of Korea. Volume 3, number 3. Chrysophyta: Bacillariophyceae: Pennales: Raphidineae: Eunotiaceae. Freshwater diatoms III. Incheon, National Institute of Biological Resources

Joh G (2012a) Algal flora of Korea. Volume 3, number 7. Chrysophyta: Bacillariophyceae: Pennales: Raphidineae: Achnanthaceae. Freshwater diatoms V. Incheon, National Institute of Biological Resources

Joh G (2012b) Algal flora of Korea. Volume 3, number 9. Chrysophyta: Bacillariophyceae: Pennales: Raphidineae: Naviculaceae: Biremis, Caloneis I, Pinnularia I. Freshwater diatoms VII. Incheon, National Institute of Biological Resources

Jones V (2013) Diatom Introduction. In: Elias S, Mock C (eds) Encyclopedia of Quaternary Science. Elsevier, pp 361–367

Kociolek P (2011) *Nitzschiaoregona*. Available at: https://diatoms.org/species/ nitzschia_oregona (Accessed 1st Feb 2022)

Krammer K, Lange-Bertalot H (1986) Bacillariophyceae: Naviculaceae. In: Ettl H, Gerloff J, Heynig H, Mollenhauer D (eds) Süsswasserflora von Mitteleuropa, Vol. 2/1, Gustav Fischer Verlag, Stuttgart

Krammer K, Lange-Bertalot H (1988) Bacillariophyceae: Bacillariaceae, Epithemiaceae, Surirellaceae. In: Ettl H, Gerloff J, Heynig H, Mollenhauer D (eds) Süsswasserflora von Mitteleuropa, Vol. 2/2, Gustav Fischer Verlag, Stuttgart

Krammer K, Lange-Bertalot H (1991a) Bacillariophyceae: Centrales, Fragilariaceae, Eunotiaceae. In: Ettl H, Gerloff J, Heynig H, Mollenhauer D (eds) Süsswasserflora von Mitteleuropa, Vol. 2/3, Gustav Fischer Verlag, Stuttgart.

Krammer K, Lange-Bertalot H (1991b) Bacillariophyceae: Achnanthaceae, Kritische Ergänzungen zu *Navicula* (Lineolatae) und *Gomphonema* Gesamtliterarurverzeichnis. In: Ettl H, Gerloff J, Heynig H, Mollenhauer D (eds) Süsswasserflora von Mitteleuropa, Vol. 2/4, Gustav Fischer Verlag, Stuttgart.

Kulikovskiy MS, Glushchenko AM, Genkal SI, Kuznetsova IV (2016) Identification book of diatoms from Russia. Yaroslavl, Filigran (in Russian)

Lange-Bertalot H, Hofmann G, Werum M, Cantonati M (2017) Freshwater Benthic Diatoms of Central Europe: Over 800 Common Species Used in Ecological Assessment. Schmitten-Oberreifenberg, Koeltz Botanical Books, English edition with updated taxonomy and added species

Lee, JH (2011) Algal flora of Korea. Volume 3, number 4. Chrysophyta: Bacillariophyceae: Pennales: Raphidineae: Naviculaceae. *Cymbella, Cymbopleura, Encyonema, Encyonopsis, Reimeria, Gomphonema*. Freshwater diatoms IV. Incheon, National Institute of Biological Resources

Lee, JH (2012) Algal flora of Korea. Volume 3, number 8. Chrysophyta: Bacillariophyceae: Pennales: Raphidineae: Naviculaceae. Freshwater diatoms VI. Incheon, National Institute of Biological Resources.

Liu J, Taniguchi H (2002) Active volcanoes in China. J Asian Stud 6:173–189

Liu J, Chu G, Han J, Rioual P, Jiao W, Wang K (2009) Volcanic eruptions in the Longgang volcanic field, northeastern China, during the past 15,000 years. J Asian Earth Sci 34:645–654

Lotter AF, Birks HJB (1993) The impact of the Laacher See Tephra on terrestrial and aquatic ecosystems in the Black Forest, southern Germany. J Quat Sci 8:263–276

Lotter AF, Birks HJB, Zolitschka B (1995) Late-glacial pollen and diatom changes in response to two different environmental perturbations: volcanic eruption and Younger Dryas cooling. J Paleolimnol 14:23–47

Lotter AF, Birks HJ, Hofmann W, Marchetto A (1998) Modern diatom, cladocera, chironomid, and chrysophyte cyst assemblages as quantitative indicators for the reconstruction of past environmental conditions in the Alps. II. Nutrients. J Paleolimnol 19:443–463

Lowe RL (2003) Keeled and canalled raphid diatoms. In: Wehr JD, Sheath RG, Kociolek JP (eds) Freshwater Algae of North America. Elsevier Science, pp 669–684

Lowe DJ (2011) Tephrochronology and its application: a review. Quat Geochronol 6(00):107–153

Lowe JJ, Walker MJC (2015) Biological Evidence. Reconstructing Quaternary Environments. Routledge, London, pp 181–266

Lund JWG (1950) Studies on *Asterionella formosa* Hass: II. nutrient depletion and the spring maximum. J Ecol 38:1–14

Mackay A, Jones V, Battarbee R (2003) Approaches to Holocene climate reconstruction using diatoms. In: Mackay A, Battarbee R, Birks J, Oldfield F (eds) Global Change in the Holocene. Routledge, London, pp 294–309

Mayr C, Smith RE, García ML, Massaferro J, Lücke A, Dubois N, Maidana NI, Meier WJH, Wissel H, Zolitschka B (2019) Historical eruptions of Lautaro Volcano and their impacts on lacustrine ecosystems in southern Argentina. J Paleolimnol 62:205–221

Metzeltin D, Lange-Bertalot H, Soninkhishig N (2009) Diatoms in Mongolia. In: Lange-Bertalot H (ed) Iconographia Diatomologica Vol. 20, Gantner ARG, Verlag KG, Ruggell pp 691

Michelutti N, Lemmen JL, Cooke CA (2015) Assessing the effects of climate and volcanism on diatom and chironomid assemblages in an Andean lake near Quito, Ecuador. J Limnol 75:274–285

Mingram J, Allen JRM, Brüchmann C, Liu J, Luo X, Negendank JFW, Nowaczyk N, Schettler G (2004) Maar- and crater lakes of the Long Gang Volcanic Field (N.E. China)—overview, laminated sediments, and vegetation history of the last 900 years. Quat Int 123–125:135–147

Mingram J, Stebich M, Schettler G, Hu Y, Rioual P, Nowaczyk N, Dulski P, You H, Opitz S, Liu Q, Liu J (2018) Millennial-scale East Asian monsoon variability of the last glacial deduced from annually laminated sediments from Lake Sihailongwan, N.E. China Quat Sci Rev 201:57–76

Mingram J, Frank U, You H, Stebich M, Liu J (2009) A widespread east Asian chronomarker (Aira-TN tephra) found in varved maar lake sediments (Sihailongwan and Erlongwan) of the Long Gang Volcanic Field (NE China). In: IAVCEI – CVS – IAS 3IMC Conference

Miyairi Y, Yoshida K, Miyazaki Y, Matsuzaki H, Kaneoka I (2004) Improved 14C dating of a tephra layer (ATtephra, Japan) using AMS on selected organic fractions. Nucl Instrum Methods Phys Res B 223/224:555–559

Ossyssek S, Geist J, Werner P, Raeder U (2020) Identification of the ecological preferences of *Cyclotella comensis* in mountain lakes of the northern European Alps. Arct Antarct Alp Res 52:512–523

Parplies J, Lücke A, Vos H, Mingram J, Stebich M, Radtke U, Han SGH (2008) Late glacial environment and climate development in northeastern China derived from geochemical and isotopic investigations of the varved sediment record from Lake Sihailongwan (Jilin Province). J Paleolimnol 40:471–487

Passy SI (2008) Continental diatom biodiversity in stream benthos declines as more nutrients become limiting. PNAS 105:9663–9667

Payne RJ, Egan J (2019) Using palaeoecological techniques to understand the impacts of past volcanic eruptions. Quat Int 499:278–289

Pla S, Anderson NJ (2005) Environmental factors correlated with chrysophyte cyst assemblages in low arctic lakes of southwest Greenland. J Phycol 41:957–974

Pla S, Camarero L, Catalan J (2003) Chrysophyte cyst relationships to water chemistry in Pyrenean lakes (NE Spain) and their potential for environmental reconstruction. J Paleolimnol 30:21–34

Reavie ED, Smol JP, Sharpe ID, Westenhofer LA, Roberts AM (2000) Paleolimnogical analyses of cultural eutrophication patterns in British Colombia lakes. Can J Bot 78:873–888

Rioual P, Morales EA, Chu G, Han J, Dong Li, Liu J, Liu Q, Mingram J, Ector L (2014) *Staurosira longwanensis* sp. nov., a new araphid diatom (Bacillariophyta) from Northeast China. Fottea 14:91–100

Rioual P, Wang L, Chu G, Gao Q, Han J, Mackay AW, Mingram J, Panizzo VN, Zhang Z,Liu J (2016) A Review on diatom records of environmental change in maar lakes of the Long Gang Volcanic Field (Northeast China). In: AVCEI – 6th International Maar Conference

Sandgren CD (1991) Chrysophyte reproduction and resting cysts: a paleolimnologist's primer. J Paleolimnol 5:1–9

Saros JE, Anderson NJ (2015) The ecology of the planktonic diatom *Cyclotella* and its implications for global environmental change studies. Biol Rev 90:522–541

Scheffler W, Morabito G (2003) Topical observations on centric diatoms (Bacillariophyceae, Centrales) of Lake Como (N. Italy). J Limnol 62:47–60

Scheffler W, Nicklish A, Schönfelder I (2005) Beiträge zur Morphologie, Ökologie und Ontogenie der planktischen Diatomee *Cyclotella comensis* Grunow. Untersuchungen an historischem und rezentem Material. Diatom Res 20(1):171–200

Schettler G, Liu Q, Mingram J, Negendank JFW (2006a) Palaeovariations in the East-Asian monsoon regime geochemically recorded in varved sediments of Lake Sihailongwan (Northeast China, Jilin Province). part 1: Hydrological conditions and dust flux. J Paleolimnol 35:239–270

Schettler G, Liu Q, Mingram J, Stebich M, Dulski P (2006b) East-Asian monsoon variability between 15000 and 2000 cal. yr BP recorded in carved sediments of Lake Sihailongwan (northeastern China, Long Gang volcanic field). Holocene 16:1043–1057

Schettler G, Romer RL, Mingram J (2004) Lake Sihailongwan – A natural monitor of dust deposition for NE-China. The Pb, Nd, and Sr isotopic record. In: AGU 2004 Fall Meeting, San Francisco, USA, 2004

Solak CN, Alakananda B, Kulikovskiy M, Blanco S, Kaleli A, Yilmaz E (2019) Distribution of nitzschioid diatoms in Kütahya waters. Oceanol Hydrobiol Stud 48:140–164

Stebich M, Arlt J, Liu Q, Mingram J (2007) Late Quaternary vegetation history of Northeast China—recent progress in the palynological investigations of Sihailongwan maar lake. CFS 259:181–190

Stebich M, Mingram J, Han J, Liu J (2009) Late Pleistocene spread of (cool-)temperate forests in Northeast China and climate changes synchronous with the North Atlantic region. Glob Planet Change 65:56–70

Stebich M, Rehfeld K, Schlütz F, Tarasov P, Liu J, Mingram J (2015) Holocene vegetation and climate dynamics of NE China based on the pollen record from Sihailongwan Maar Lake. Quat Sci Rev 124:275–289

Telford RJ, Barker P, Metcalfe S, Newton A (2004) Lacustrine responses to tephra deposition: examples from Mexico. Quat Sci Rev 23:2337–2353

Urrutia R, Araneda A, Cruces F, Torres L, Chirinos L, Treutler HC, Fagel N, Bertrand S, Alvial I, Barra R, Chapron E (2007) Changes in diatom, pollen, and chironomid assemblages in response to a recent volcanic event in Lake Galletué (Chilean Andes). Limnologica 37:49–62

Van Dam H, Mertens A, Sinkeldam JA (1994) Coded checklist and ecological indicator values of freshwater diatoms from The Netherlands. Neth J Aquat Ecol 28:117–133

Wang X, Qiu S, Song C, Kulakov A, Tashchi S, Myasnikov E (2001) Cenozoic volcanism and geothermal resources in northeast China. Chin Geogr Sci 11:150–154

Wentzky VC, Tittel J, Jäger CG, Bruggeman J, Rinke K (2020) Seasonal succession of functional traits in phytoplankton communities and their interaction with trophic state. J Ecol 108:1649–1663

Wetzel CE, Ector L (2015) Taxonomy and ecology of *Fragilaria microvaucheriae* sp. nov. and comparison with the type materials of *F. uliginosa* and *F. vaucheriae*. Cryptogam, Algol 36:271–289

Wu J, Zhu Z, Sun C, Rioual P, Chu G, Liu J (2019) The significance of maar volcanoes for palaeoclimatic studies in China. J Volcanol Geotherm Res 383:2–15

Wutke K, Wulf S, Tomlinson EL, Hardiman M, Dulski P, Luterbacher J, Brauer A (2015) Geochemical properties and environmental impacts of seven Campanian tephra layers deposited between 40 and 38 ka BP in the varved lake sediments of Lago Grande di Monticchio, southern Italy. Quat Sci Rev 118:67–83

Yan B (1998) Geochemical features of aquatic environment in crater and barrier lakes in northeast of China. Chin Geogr Sci 8:352–361

Zhao H, Hall VA (2015) Assessing the potential for cryptotephra studies in Northeastern China. Holocene 25:772–783

Zhao H, Liu J, Hall VA, Li X (2017) Tephrostratigraphical investigation of lake sediments and a peat bog in northeastern China since 20,000 years. Holocene 27:765–778

Zhu J, Mingram J, Brauer A (2013) Early Holocene aeolian dust accumulation in northeast China recorded in varved sediments from Lake Sihailongwan. Quat Int 290–291:299–312

Zhu Z, Wu J, Rioual P, Mingram J, Yang H, Zhang B, Chu G, Liu J (2021) Evaluation of the sources and seasonal production of brGDGTs in Lake Sihailongwan (N.E. China) and application to reconstruct paleo-temperatures over the period 60–8 ka BP. Quat Sci Rev 261:1–11